Multiple solvent signal presaturation and decoupling artifact removal in 13C1H nuclear magnetic resonance

Marine Canton, Richard Roe, Stéphane Poigny, Jean-Hugues Renault, Jean-Marc Nuzillard

Multiple solvent signal presaturation in ^{13}C NMR

M. Canton[1,2], R. Roe[2], S. Poigny[2], J.–H. Renault[1], and J.–M. Nuzillard[1]

[1]Université de Reims Champagne Ardenne, CNRS, ICMR UMR 7312, 51097 Reims, France
[2]Laboratoires Pierre Fabre Dermocosmétique, 3 Avenue Hubert Curien, BP 13562, 31035 Toulouse Cedex, France

Correspondence: M. Canton (marine.canton@univ-reims.fr)

Abstract. The analysis by proton-decoupled carbon-13 nuclear magnetic resonance (^{13}C{^{1}H} NMR) of samples dissolved in solvents presenting strong multiple resonances can be facilitated by the suppression of these resonances by multi–site presaturation. The benefit of this operation is the elimination of the possible artifacts that arise from the solvent signals in non-optimized decoupling conditions. On the five solvents studied (glycerol, 1,2–propanediol, 1,3–propanediol, 1,2–butanediol, 1,3–butanediol), the simultaneous presaturation of two, three and four signals causes a decrease of more than 94% on a narrow window (50% decrease on a window of less than 50 Hz). In the case of frequency close solvent resonances, the experimental measurement of the width of signal suppression zones leads to unexpected selectivity profiles. The origin of this observation was ascertained by means of computer calculations for the resolution of the Bloch equations during multi–site presaturation.

1 Introduction

Nuclear magnetic resonance (NMR) spectroscopy is the reference technique for structural elucidation. Because it is a non-destructive method, for each probe, a signal of each selected atom is detected. In some cases, the sample is strongly diluted in a solvant (e.g. 55M for water and few mM for proteins) (Zheng and Price, 2010). Thus, signals can be interfere because they overlap with the resonance of interest or they saturate the NMR receiver causing complications such as baseline distortions. For this reason, many solvent signal suppression techniques have been and continue to be developed in ^{1}H analyses (Lee et al., 2017; Chen et al., 2017; Duarte et al., 2013; Gouilleux et al., 2017). Most of the time, the water or the ethanol are the problematic solvents, as the method "Watergate" designed specifically for suppressing water signals (Friedbolin, 2011; Kew et al., 2017). For example, in the case of protein study, the water suppression is mandatory to allow full utilization of receiver dynamic range and enable the maximal sensitivity (Mo and Raftery, 2008).

Solvent signal suppression methods are based on modifications in the pulse sequence or in the post-processing. Unfortunately, these methods are not limited to the suppression of the solvent resonances but rather decrease the intensity of a range of frequencies (Zheng and Price, 2010). The goal is to have a signal suppression window as small as possible in order not to lose the detection of signals of interest. Among all the signal suppression techniques, the presaturation consists of applying a low-power selective radiofrequency (RF) irradiation on the solvent resonances during the relaxation delay (Hoult, 1976)

(Ross et al., 2007). Multisite presaturation in a way already employed in ^{1}H NMR for the analysis of alcoholic beverages. The eight ^{1}H NMR frequencies of water and ethanol, from the hydroxy, methylene, and methyl group, must be suppressed when dealing with such samples (Monakhova et al., 2011).

In this work, our aim is to suppress solvent signals in ^{13}C NMR analysis. Indeed, the ^{13}C NMR analysis is a widely used technique to characterize compounds in natural extracts (Hubert et al., 2014) (Tsujimoto et al., 2018) (Bakiri et al., 2017). Plant extracts may be conditioned as dry products or as solutions in diverse solvents, possibly prepared from renewable resources and for which evaporation to dryness may not feasible or nor compatible with the chemical integrity of the solutes. Alcohols like glycerol, propanediols, butanediols and pentanediols are employed for such applications (Chemat et al., 2019) (Shehata et al., 2015). The characterization of the solutes by ^{13}C NMR spectroscopy may be carried out on extracts or on fractions obtained by chromatographic methods. It may happen that fractions of interest also contain an important amount of these high boiling point solvents.

The presence of high intensity resonances from solvents is not a problem in ^{13}C NMR spectroscopy most of times since their resonance lines are very sharp. However, NMR data acquisition of series of samples is often achieved in automation mode and standard acquisition parameters are used for this purpose. Since ^{13}C ^{1}H spectra are recorded, the calibration of pulses is necessary on the ^{1}H channel for proper decoupling. Decoupling pulse miscalibration may cause decoupling artifacts around the intense solvent signals to, at a point their intensity is comparable to the one of the signals of interest (Blechta and Schraml, 2015). The problem was solved by reducing the intensity of solvent signals by multisite presaturation. For this purpose, we used the Shifted Laminar Pulses (SLP) method to target multiple frequencies to saturate. In the article “Single- and Multiple-Frequency- Shifted Laminar Pulses”, S. Patt explained how to place the centre of an or several excitations at a location other than the receiver. Instead of moving the frequency source by the desired amount, which can cause problems of phase coherence, the method consists in define laminar pulses which are sequential amplitude- and phase- modulated rectangular pulses (Patt, 1992).

During the assessment of the method, the measurement of the width of the signal suppression zone produced an unexpected result when the saturation of frequency close resonances was necessary. The apparent "interference" effect between saturation pulses recalled the one observed for two closely frequency-shifted BURP pulses, as reported in the article entitled "Close encounters between soft pulses" (Kupče and Freeman, 1995). In this article, E. Kupce and R. Freeman demonstrated that an intermediate separation of two resonances ($6 > \Delta F/\ \Delta f > 2$) brings “waves” disruptions while smaller separations ($\Delta F\ /\ \Delta f < 2$) engenders disintegrated profiles in the magnetization trajectories. A numerical simulation of multisite resonance saturation was therefore undertaken in order to interpret this result. In a first part, we will present the theory of presaturation that led to the writing of the numerical simulation as well as the results obtained. Experimental results are then exposed. We studied the presaturation of glycerol by suppressing one then simultaneously its two signals and measuring the signal window suppression. Then, with an example of sucrose heavily diluted in the glycerol, we will observe artifacts and how the presaturation of the signals of the solvent removes these and allows the analysis of the sample. Finally, the results of presaturation on two to four signals of glycols propane–1,2–diol, propane–1,3–diol, butane–1,2–diol and butane–1,3–diol will be demonstrated.

2 Theory

Resonance saturation in NMR occurs when an RF field is applied continuously at a frequency equal to the resonance frequency of a nucleus. The magnetization dynamics of a collection of many identical isolated spins that constitutes a macroscopic sample is governed by the Bloch equations (Bloch, 1946). The components M_x, M_y, and M_z of the macroscopic magnetization $\boldsymbol{M}$, when observed in the rotating frame of reference, evolve as follows,

$$\begin{aligned}
\frac{dM_x}{dt} &= \Omega_0 M_y - \Omega_{1y} M_z - R_2 M_x \\
\frac{dM_y}{dt} &= \Omega_{1x} M_z - \Omega_0 M_x - R_2 M_y \\
\frac{dM_z}{dt} &= \Omega_{1y} M_x - \Omega_{1x} M_y - R_1 (M_z - M_z^{\mathrm{eq}})
\end{aligned} \tag{1}$$

in which Ω_0 is the precession angular frequency, Ω_1 is the norm of the nutation angular frequency vector, and Ω_{1x} and Ω_{1y} the components of the latter on the X and Y axis of the rotating frame. Nuclear spin relaxation is phenomenologically described by the two rate constants R_1 and R_2 defined as the reciprocals of the longitudinal and transverse relaxation times T_1 and T_2, respectively. M_z^{eq} denotes the value of the sample equilibrium nuclear magnetization and intervenes in the description of the longitudinal relaxation. In the case $\Omega_0 = 0$ of an on-resonance constant intensity RF field, the components of the magnetization vector tend toward a stationary limit for which

$$M_z^{\mathrm{stat}} = \frac{M_z^{\mathrm{eq}}}{1 + \Omega_1^2 T_1 T_2} \tag{2}$$

If $\Omega_1^2 T_1 T_2 \gg 1$, then the stationary magnetization is much lower than the one of equilibrium, corresponding to an equalization of spin state populations induced by the RF field, as expected from saturation.

Solvent signal suppression in NMR spectroscopy can be obtained by selective saturation of one or more solvent signals during the relaxation delay. This pulse sequence period is named presaturation because it precedes the non–selective excitation of the sample resonances. Presaturation at a single site is easily achieved by continuous wave RF irradiation. Multisite presaturation relies on multiple–frequency–shifted laminar pulses, a particular species of shaped pulse (Patt, 1992). Such a shaped pulse serves as presaturation module of duration T and is applied repetitively to the sample so that the overall RF irradiation time is equal to the desired relaxation delay. A presaturation module is constituted by N elementary pulses, named slices hereafter, of duration δt so that $T = N\delta t$. In Figure 1, the experimental sequence is presented. The creation of a module requires the definition of T, N, of the number n of presaturation sites, and of the list of the frequency offsets Ω_k^{sat} associated to each site. The values of Ω_{1x} and Ω_{1y} are obtained from

$$(\Omega_{1x} + i\Omega_{1y})(t_j) = \frac{\Omega_1}{n} \sum_{k=0}^{n-1} \exp(i\Omega_k^{\mathrm{sat}} \cdot j\delta t) \quad \text{for} \quad 0 \leq j < N \tag{3}$$

which states that RF field intensities are equally distributed among the n sites and phases arbitrarily are set to zero at $t = 0$.

The Ω_k^{sat} values are calculated relatively to an auxiliary carrier frequency determined as the average of the highest and the lowest offsets of the signals to presaturate. The emission of the presaturation pulse has to take into account the difference

between the auxiliary frequency and the actual transmitter frequency, the so–called shaped pulse offset, as described in Fig. 2. The value of δt is chosen so that the highest precession angle $|\Omega_k^{\rm sat}|\delta t$ for the highest $|\Omega_k^{\rm sat}|$ must be kept below a small threshold value in the order of $\pi/15$. The value of N should be as high as possible and depends on the memory size available for shaped pulses in the pulse program sequencer. N = 50,000 was used throughout the present study. The $N\delta t$ product determines the shaped pulse duration T. Alternatively, T may be chosen so that the highest precession angle falls under the predefined threshold for the retained value of N.

The simulation of an experimental set of spectra like the one in Fig. 3 requires first the creation of a table of N values of Ω_{1x} and of Ω_{1y} according to Eqn. (3). Nucleus resonance offset frequencies $\Omega_0/2\pi$ are then repetitively selected for presaturation effect calculation from a set of linearly spaced values comprised between a minimum and a maximum. Starting from a magnetization vector in its equilibrium position, the action it undergoes from the series of presaturation modules is evaluated. The offset frequency and final amount of longitudinal magnetization M_z are directed to a computer file so that a graph of $M_z(\Omega_0/2\pi)$ can be drawn for the chosen set of Ω_0 values. The action of a presaturation module is determined by the action of the series of its constituting slices. The action of each shaped pulse slice should be calculated by resolution of the Bloch equation system (Eqn. 1) over duration δt, even though a different method was adopted, as explained hereafter.

Exact solutions of the Bloch equations have been reported but bear some degree of complexity (Canet et al., 1994; Madhu and Kumar, 1995). They take simultaneously account for magnetization precession, nutation and relaxation processes. The approach adopted here makes use of an easy to implement approximate solution. It relies on the observation that magnetization evolution induced by relaxation alone is slow compared to the one induced by simultaneous precession and nutation. The evolution of $\boldsymbol{M}$ solely under precession and nutation resumes to a rotation at angular frequency $\Omega^{\rm eff}$, the norm of vector $\mathbf{\Omega^{eff}}(\Omega_{1x},\Omega_{1y},\Omega_0)$ when reported in the rotating frame of reference. The rotation axis is defined by the unitary vector $\boldsymbol{u} = \mathbf{\Omega^{eff}}/\Omega^{\rm eff}$. For practical calculations, one need to express the elements of the rotation matrix $\mathbf{R}_{\boldsymbol{u},\theta}$ in which $\theta = \Omega^{\rm eff}\delta t$ and $\boldsymbol{u}(u_x,u_y,u_z)$.

$$\mathbf{R}_{\boldsymbol{u},\theta} = \cos\theta \begin{pmatrix} 1 & 0 & 0 \\ 0 & 1 & 0 \\ 0 & 0 & 1 \end{pmatrix} + (1-\cos\theta) \begin{pmatrix} u_x^2 & u_xu_y & u_xu_z \\ u_xu_y & u_y^2 & u_yu_z \\ u_xu_z & u_yu_z & u_z^2 \end{pmatrix} + \sin\theta \begin{pmatrix} 0 & -u_z & u_y \\ u_z & 0 & -u_x \\ -u_y & u_x & 0 \end{pmatrix} \tag{4}$$

Relaxation alone is taken account by the following transformation of $\boldsymbol{M}$.

$$(M_x, M_y, M_z) \longrightarrow (M_x e^{-R_2\delta t}, M_y e^{-R_2\delta t}, M_z^{\rm eq} + (M_z - M_z^{\rm eq})e^{-R_1\delta t}) \tag{5}$$

The evolution of $\boldsymbol{M}$ during a time slice of duration δt is simply calculated by the successive application of rotation and relaxation transformations. The approximation that consists in alternating rotation and relaxation instead of considering them simultaneously improves when δt tends to zero. A given δt time interval can be divided in two (or more) parts and the replacement of rotation(δt)–relaxation(δt) by two consecutive rotation($\delta t/2$)–relaxation($\delta t/2$) calculations provides a way to evaluate the error induced by the proposed calculation method.

An identical approach to Bloch equations resolution was used for the re–optimization of band–selective uniform response pulses (BURP) in the presence of relaxation, leading to the design of pulses with silhouette largely unaffected by relaxation

processes (SLURP), for which the underlying technical details were not disclosed (Nuzillard and Freeman, 1994). The action of relaxation on frequency–domain profiles of BURP pulses were recalculated using exact solutions of the Bloch equations and the results were visually identical to those derived from the approximate treatment (Canet et al., 1994).

The simulation computer source code was written in C language; it relied on the libxml2 library for the reading of the input data file (this may be an overkill for such a task, admittedly) and on the libsimu1 library for the calculation of rotation matrices by means of Eqn. (4), as programmed for the design of SLURP pulses. The libsimu1 archive file also contains a proof of Eqn. (4). The computer code for saturation simulations is available from GitHub; its installation was tested with Cygwin under Windows 10 but should be easily carried out on any other platform that provides a C compiler and UNIX–like tools.

3 Results

Suppression of solvent signals with the presaturation technique was the key to characterize sample diluted in it. The experimental way to trace out the profile of a multisite presaturation is to select a resonance to be suppressed, to vary the shaped pulse offset, and to draw the corresponding peaks produced by the pulse sequence in Fig. 1. The minimal two–step phase program ensures that peaks are all identically phased and that their heights are proportional to the amount of longitudinal magnetization present at the end of the presaturation period. The first experimental trial of glycerol ^{13}C resonances suppression worked as expected. Indeed, the glycerol, formula $C_3H_8O_3$, has two ^{13}C signals due to its symmetry at δ_A = 63.5 ppm and δ_B = 72.9 ppm. When, the presaturation at the single site was applied with a continuous wave RF irradiation to the precise resonance $\Omega_A/2\pi$ = 9,613 Hz, we observed a suppression of the signal of 97%. Moreover, simultaneous presaturation of the two signals $\Omega_A/2\pi$ = 9,613 Hz and $\Omega_B/2\pi$ = 11,037 Hz led to a significant attenuation of more than 95% of both signals, as shown in Figure 4.

Experimental presaturation profiles were measured in order to evaluate the width of the frequency band concerned by signal attenuation. For this purpose, about one hundred experiments were carried out on each signal by varying the auxiliary frequency associated to each site in intervals of 1 Hz. Then, by integrating the signals, we can measure the window for which 50% of the initial signal intensity is removed. More precisely, the profile of the signal A presents a bell shape whose width at half height was 15 Hz for $\Omega_1/2\pi$ = 250 mHz, that represents 0.1 ppm at 151 MHz (Figure 5). Similarly, for the signal B, the half reduction of the signal is observed over a width of 14 Hz equivalent to 0.09 ppm at 151 MHz. The profiles obtained are those expected and observed for a multisite presaturation of two large-scale resonances (in our case $\Omega_B/2\pi - \Omega_A/2\pi$ = 1,424 Hz). Moreover, these narrow windows of attenuation signals demonstrate that there is no loss of signal information around presaturation frequencies. This information is important for the analyses of sample diluted in glycerol. The power of RF pulses emitted during presaturation is a component of the residual longitudinal magnetization Mz and therefore the intensity of the signal obtained. The power must be very low to reach a suppression of the signal. Five experiments were carried out by varying only the power of RF pulses starting at a power of 1 mW and dividing by 2 to reach 0.01 mW. The intensity of the two residual signals were similar: signals attenuations for the fixed experiments were at least 95%. Based on these results, we have retained the power used in previous experiments, 0.04 mW, for future presaturation analyses.

The following study involves the analysis of a solution of sucrose (24 mM) in DMSO–d_6 containing glycerol in high proportion (3.6 M). This sample represents a real case in the sense that plant extracts can be heavily diluted in matrices like glycerol and the concentration of the metabolites are close to than our model sample. The ^{13}C NMR spectrum of this sample compared to the ^{13}C NMR spectrum of sucrose in DMSO–d_6 is presented in Figure 6. In the ^{13}C NMR spectrum of sucrose, the twelve carbon signals appear between $\delta = 60$ ppm and $\delta = 104$ ppm. In the ^{13}C NMR spectrum of the sucrose diluted in glycerol sample, some signals should not appear. Indeed, in addition to the twelve sucrose signals and the two glycerol signals, we can easily observe artifacts (or "ghost signals") generated by the high concentration of glycerol. Some artifact signals have abnormal phases while others may be confused with signals of interest and complicate the characterization of unknown samples. The first studied hypothesis for the presence of these "ghost signals" was the receptor saturation. Generally, the presence of large solvent signals requires a low receiver gain (Zheng and Price, 2010), but as the modification of receiver gain doesn't change artifact chemical shifts, the hypothesis of their cause was refuted. This parameter was setting at its maximum (RG = 2,000) for all the experiments in order to have a good sensibility for minor compounds diluted in the sample. The second hypothesis was the ^{1}H broad-band decoupling. In practise, ^{13}C{^{1}H} decoupling is performed during the entire ^{13}C data acquisition period by irradiations (Friedbolin, 2011). Thus, the calibration of pulses is necessary on the ^{1}H channel for proper decoupling. As thought, modifications on the decoupling pulse parameters caused the movement of artifacts on the NMR spectrum. The hypothesis is verified: the intense solvent signals cause decoupling pulse miscalibration occasioning the presence of decoupling artifacts around these signals. Because decoupling artifacts refer to electronics, analysing the same sample several times does not cause artifacts at the same chemical shifts. This observation refutes that the knowledge of the artifacts chemical shifts on the ^{13}C NMR spectrum of a high proportion glycerol-containing sample allows us to know studied sample chemical shifts. The problem was solved thanks to the presaturation in ^{13}C NMR. As observed in Figure 6, reducing the intensity of solvent signals by multiple presaturation removes decoupling artifacts. With this technique, signals observed on the NMR spectrum belong to the compounds present in the sample. Obviously, the matrix effect generated chemical shifts about 0.3 ppm for some signals, but the characterization of the sample was achievable. At present, the proof of concept was carried out on more than 20 samples of natural extracts diluted in glycerol.

Multiple site presaturation was extended to other heavy solvents used as natural extracts matrices: 1,2–propanediol, 1,3–propanediol, 1,2–butanediol and 1,3–butanediol containing two to four resonance frequencies in ^{13}C NMR. For the three latter, the presaturation permits, as expected, an elimination of more than 94% of the signals. The more signals to presaturate there are, the lower is the RF field B_1 and the greater the attenuation is generated. Moreover, as we can see in the table, their widths of the frequency band concerned by signal attenuation are narrow between 5 Hz to 11 Hz for 1,2–butanediol. However, it is not impossible that a signal of interest will be included in this window and deleted. In this case, the signals of the other carbons present in the compound will still allow its characterization.

The elimination of the ^{13}C resonances of 1,2–propanediol led to an unexpected presaturation profile in the region of two oxygen–bearing carbons, due to their very close chemical shift values (δ_B = 67.8 ppm and δ_C = 67.9 ppm). The profile showed puzzling irregular features that indeed motivated the undertaking of the numerical simulation work. In this case $\Omega_C^{sat}/2\pi$ – $\Omega_B^{sat}/2\pi$ = 10 Hz. The simulated profiles f in Figure 3, corresponding to 10 Hz offset, have similarities with the experimental

profile. Indeed, the same wave effect is observed around more or less 40 Hz of the resonance studied, Figure 7 shows the saturation profile for these two resonances between more or less 50 Hz of their exact frequencies.

The automatisation of the suppression was reached for the five studied solvents creating a macro for each in the acquisition software. Specifying chemical shift windows of 1 ppm, the macro automatically determines the exact solvent frequencies in a reference measurement. It creates the presaturation modules varying the shaped pulse offset and selected the Ω^{sat} corresponding. It launches the acquisition and the fourier transform. For the 1,2–propanediol, the two close frequencies brang some problems to the macro determine the solvent frequencies. A way to cleanly presaturate two close frequency resonances is to target their average offset with a double saturation field intensity. The macro, written in C language, used to presaturate glycerol is available on the libsimu1 library.

4 Experimental

Glycerol, 1,2–propanediol, 1,3–propanediol, 1,2–butanediol and 1,3–butanediol were prepared diluting 200 mg of each in 0.6 mL of DMSO–d_6. This corresponds to sample with high concentration: 3.62 M for glycerol, 4.38 M for propanediols and 3.70 M for butanediols. Glycerin was kindly given by Pierre Fabre Dermocosmétiques. 1,2–propanediol and D(+)Saccharose were purchased from VWR. 1,3–propanediol and 1,3–butanediol were purchased from Alfa Aesar. 1,2–butanediol, was purchased from Sigma Aldrich. The sample containing sucrose (29 mM), glycerol (3.62 M) in in 0.6 mL of DMSO–d_6 was left overnight at room temperature for its complete dilution.

All experiments were performed at 298 K on a Bruker Avance AVIII-600 spectrometer (Karlsruhe, Germany) equipped with a cryoprobe optimized for ^{1}H detection and with cooled ^{1}H, ^{13}C, and two-dimensional (2D) coils and preamplifiers. ^{13}C NMR spectra were acquired at 150.91 MHz. Automated locking and shimming was done on each sample using the standard Bruker routines lock and topshim.

5 Conclusions

The present work provides a method for the saturation of intense solvent resonances in ^{13}C NMR spectroscopy, as those occurring during the analysis of complex plant extracts prepared in high boiling point solvents. Numerical simulation therefore helped us to understand the origin of unexpected presaturation profile related to the saturation of frequency close resonances, even though it does not take into account neither instrumental shortcomings such as $\mathbf{B}_0$ and $\mathbf{B}_1$ field inhomogeneities nor incomplete relaxation between transient signal recordings. The evolution of the sample magnetization was determined through the use of a simple approximation for the resolution of the Bloch equations that might find applications in other contexts. This approach opens up perspectives on signal suppression in other dilution solvents or in ^{13}C quantitative analysis of diluted extract in high boiling solvents.

Code and data availability. The PresatSimul source code is available from https://github.com/nuzillard/PresatSimul.

The libsimu1 source code is available from https://github.com/nuzillard/Libsimu1.

Author contributions. MC carried out the sample preparation and the recording of NMR spectra. JMN wrote the computer code for the simulation of presaturation and prepared the manuscript. RR, SP, and JHR contributed to the final version of the manuscript.

Competing interests. The authors declare that they have no conflict of interest.

Acknowledgements. MC thanks the Laboratoires Pierre Fabre Dermocosmétique for financial support. Financial support by CNRS, Conseil Régional Champagne Ardenne, Conseil Général de la Marne, Ministry of Higher Education and Research (MESR) and EU-programme FEDER to the PlAneT CPER project is gratefully acknowledged.

References

Bakiri, A., Hubert, J., Reynaud, R., Lanthony, S., Harakat, D., Renault, J.-H., and Nuzillard, J.-M.: Computer-Aided 13C NMR Chemical Profiling of Crude Natural Extracts without Fractionation, Journal of Natural Products, 80, 1387–1396, https://doi.org/10.1021/acs.jnatprod.6b01063, pMID: 28414230, 2017.

Blechta, V. and Schraml, J.: NMR artifacts caused by decoupling of multiple-spin coherences: improved SLAP experiment, Magnetic Resonance in Chemistry, 53, 460–466, https://doi.org/10.1002/mrc.4221, https://onlinelibrary.wiley.com/doi/abs/10.1002/mrc.4221, 2015.

Bloch, F.: Nuclear Induction, Phys. Rev., 70, 460–474, https://doi.org/10.1103/PhysRev.70.460, https://link.aps.org/doi/10.1103/PhysRev.70.460, 1946.

Canet, D., Roumestand, C., and Boubel, J.-C.: A general computer program for calculating selectivity profiles in NMR spectroscopy, Proceedings - Indian Academy of Sciences Chemical Sciences, 106, 1449 – 1462, 1994.

Chemat, F., Abert-Vian, M., Fabiano-Tixier, A. S., Strube, J., Uhlenbrock, L., Gunjevic, V., and Cravotto, G.: Green extraction of natural products. Origins, current status, and future challenges, TrAC Trends in Analytical Chemistry, 118, 248 – 263, https://doi.org/https://doi.org/10.1016/j.trac.2019.05.037, http://www.sciencedirect.com/science/article/pii/S0165993619300706, 2019.

Chen, J., Zheng, G., and Price, W. S.: A new phase modulated binomial-like selective-inversion sequence for solvent signal suppression in NMR, Magnetic Resonance in Chemistry, 55, 115–119, https://doi.org/10.1002/mrc.4505, https://www.onlinelibrary.wiley.com/doi/abs/10.1002/mrc.4505, 2017.

Duarte, C. J., Colnago, L. A., de Vasconcellos Azeredo, R. B., and Venâncio, T.: Solvent Suppression in High-Resolution 1H NMR Spectroscopy Using Conventional and Phase Alternated Continuous Wave Free Precession, Applied Magnetic Resonance, 44, 1265–1280, https://doi.org/10.1007/s00723-013-0482-6, https://doi.org/10.1007/s00723-013-0482-6, 2013.

Friedbolin, H.: Basic One- and Two-Dimensional NMR Spectroscopy, Wiley-VCH, 5th edn., 2011.

Gouilleux, B., Charrier, B., Akoka, S., and Giraudeau, P.: Gradient-based solvent suppression methods on a benchtop spectrometer, Magnetic Resonance in Chemistry, 55, 91–98, https://doi.org/10.1002/mrc.4493, https://onlinelibrary.wiley.com/doi/abs/10.1002/mrc.4493, 2017.

Hoult, D.: Solvent peak saturation with single phase and quadrature fourier transformation, Journal of Magnetic Resonance (1969), 21, 337 – 347, https://doi.org/https://doi.org/10.1016/0022-2364(76)90081-0, http://www.sciencedirect.com/science/article/pii/0022236476900810, 1976.

Hubert, J., Nuzillard, J.-M., Purson, S., Hamzaoui, M., Borie, N., Reynaud, R., and Renault, J.-H.: Identification of Natural Metabolites in Mixture: A Pattern Recognition Strategy Based on 13C NMR, Analytical Chemistry, 86, 2955–2962, https://doi.org/10.1021/ac403223f, https://doi.org/10.1021/ac403223f, pMID: 24555703, 2014.

Kew, W., Bell, N. G., Goodall, I., and Uhrín, D.: Advanced solvent signal suppression for the acquisition of 1D and 2D NMR spectra of Scotch Whisky, Magnetic Resonance in Chemistry, 55, 785–796, https://doi.org/10.1002/mrc.4621, https://onlinelibrary.wiley.com/doi/abs/10.1002/mrc.4621, 2017.

Kupče, E. and Freeman, R.: Close Encounters between Soft Pulses, Journal of Magnetic Resonance, Series A, 112, 261 – 264, https://doi.org/10.1006/jmra.1995.1043, http://www.sciencedirect.com/science/article/pii/S1064185885710431, 1995.

Lee, D., Chaudhari, S. R., and Paëpe, G. D.: Solvent signal suppression for high-resolution MAS-DNP, Journal of Magnetic Resonance, 278, 60 – 66, https://doi.org/https://doi.org/10.1016/j.jmr.2017.03.012, http://www.sciencedirect.com/science/article/pii/S1090780717300733, 2017.

Madhu, P. and Kumar, A.: Direct Cartesian-Space Solutions of Generalized Bloch Equations in the Rotating Frame, Journal of Magnetic Resonance, Series A, 114, 201 – 211, https://doi.org/10.1006/jmra.1995.1127, http://www.sciencedirect.com/science/article/pii/S1064185885711278, 1995.

Mo, H. and Raftery, D.: Pre-SAT180, a simple and effective method for residual water suppression, Journal of Magnetic Resonance, 190, 1 – 6, https://doi.org/https://doi.org/10.1016/j.jmr.2007.09.016, http://www.sciencedirect.com/science/article/pii/S1090780707002832, 2008.

Monakhova, Y. B., Schäfer, H., Humpfer, E., Spraul, M., Kuballa, T., and Lachenmeier, D. W.: Application of automated eightfold suppression of water and ethanol signals in 1H NMR to provide sensitivity for analyzing alcoholic beverages, Magnetic Resonance in Chemistry, 49, 734–739, https://doi.org/10.1002/mrc.2823, https://onlinelibrary.wiley.com/doi/abs/10.1002/mrc.2823, 2011.

Nuzillard, J.-M. and Freeman, R.: Band-Selective Pulses Designed to Accommodate Relaxation, Journal of Magnetic Resonance, Series A, 107, 113 – 118, https://doi.org/10.1006/jmra.1994.1056, http://www.sciencedirect.com/science/article/pii/S1064185884710564, 1994.

Patt, S. L.: Single- and multiple-frequency-shifted laminar pulses, Journal of Magnetic Resonance (1969), 96, 94 – 102, https://doi.org/10.1016/0022-2364(92)90289-J, http://www.sciencedirect.com/science/article/pii/002223649290289J, 1992.

Ross, A., Schlotterbeck, G., Dieterle, F., and Senn, H.: Chapter 3 - NMR Spectroscopy Techniques for Application to Metabonomics, in: The Handbook of Metabonomics and Metabolomics, edited by Lindon, J. C., Nicholson, J. K., and Holmes, E., pp. 55 – 112, Elsevier Science B.V., Amsterdam, https://doi.org/https://doi.org/10.1016/B978-044452841-4/50004-7, http://www.sciencedirect.com/science/article/pii/B9780444528414500047, 2007.

Shehata, E., Grigorakis, S., Loupassaki, S., and Makris, D. P.: Extraction optimisation using water/glycerol for the efficient recovery of polyphenolic antioxidants from two Artemisia species, Separation and Purification Technology, 149, 462 – 469, https://doi.org/https://doi.org/10.1016/j.seppur.2015.06.017, http://www.sciencedirect.com/science/article/pii/S1383586615300423, 2015.

Tsujimoto, T., Yoshitomi, T., Maruyama, T., Yamamoto, Y., Hakamatsuka, T., and Uchiyama, N.: 13C-NMR-based metabolic fingerprinting of Citrus-type crude drugs, Journal of Pharmaceutical and Biomedical Analysis, 161, 305 – 312, https://doi.org/https://doi.org/10.1016/j.jpba.2018.08.044, http://www.sciencedirect.com/science/article/pii/S0731708518308033, 2018.

Zheng, G. and Price, W. S.: Solvent signal suppression in NMR, Progress in Nuclear Magnetic Resonance Spectroscopy, 56, 267 – 288, https://doi.org/https://doi.org/10.1016/j.pnmrs.2010.01.001, http://www.sciencedirect.com/science/article/pii/S007965651000021X, 2010.

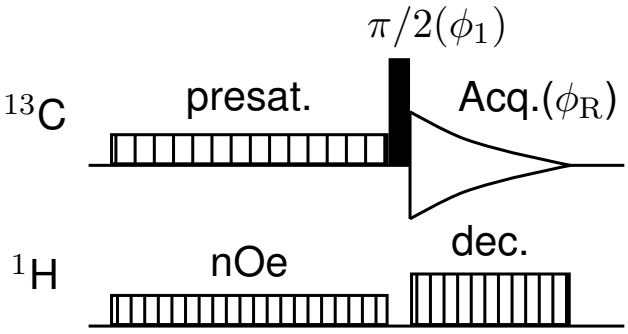

Figure 1. Pulse sequence for the recording of ^{13}C{^{1}H} spectra with sensitivity enhancement by nuclear Overhauser effect magnetization transfer from ^{1}H nuclei and with presaturation of solvent resonances. The minimal phase program is $\phi_1 = \phi_{\rm R} = (0, \pi)$.

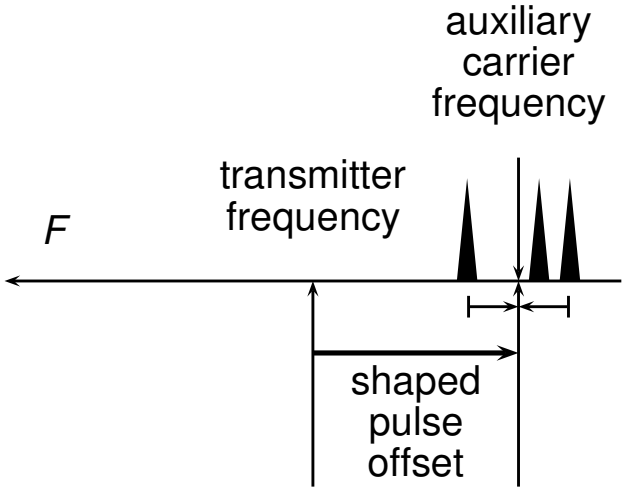

Figure 2. Definition of the offset of the presaturation shaped pulses. The narrow black triangles represent the solvent peaks. The auxiliary carrier frequency is defined as the mean of the highest and lowest solvent resonance frequencies. The offset of the presaturation shaped pulses is the difference between the auxiliary carrier frequency and the actual transmitter frequency.

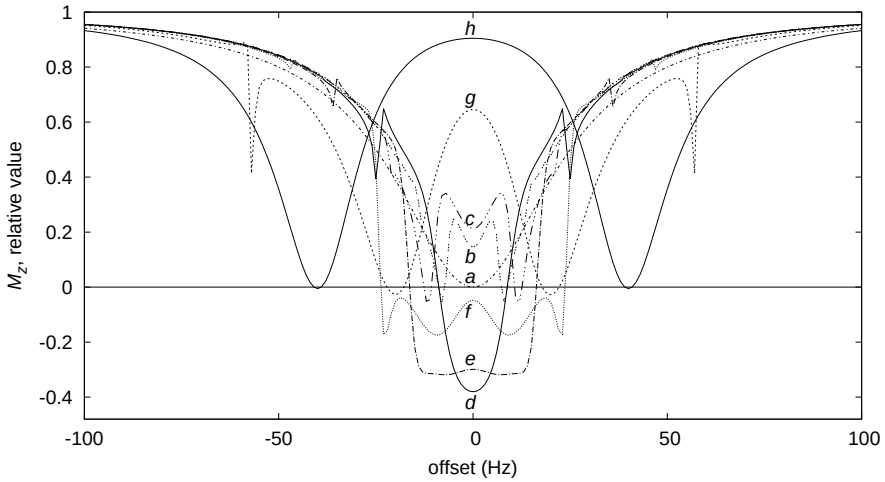

Figure 3. Saturation profiles for presaturation at two sites , at $\pm\Omega^{\mathrm{sat}}/2\pi$ for $\Omega^{\mathrm{sat}}/2\pi = 0, 2, 4, 6, 810, 20, 40$ Hz, corresponding to traces a to h. The relaxation times T_1 and T_2 are both equal to 0.5 s. The relaxation delay lasts 5 s during which 10 presaturation modules of 0.5 s each are applied. Each module is made of 50000 slices, for which Ω_{1x} and Ω_{1y} values are calculated with $\Omega_1/2\pi = 50$ Hz.

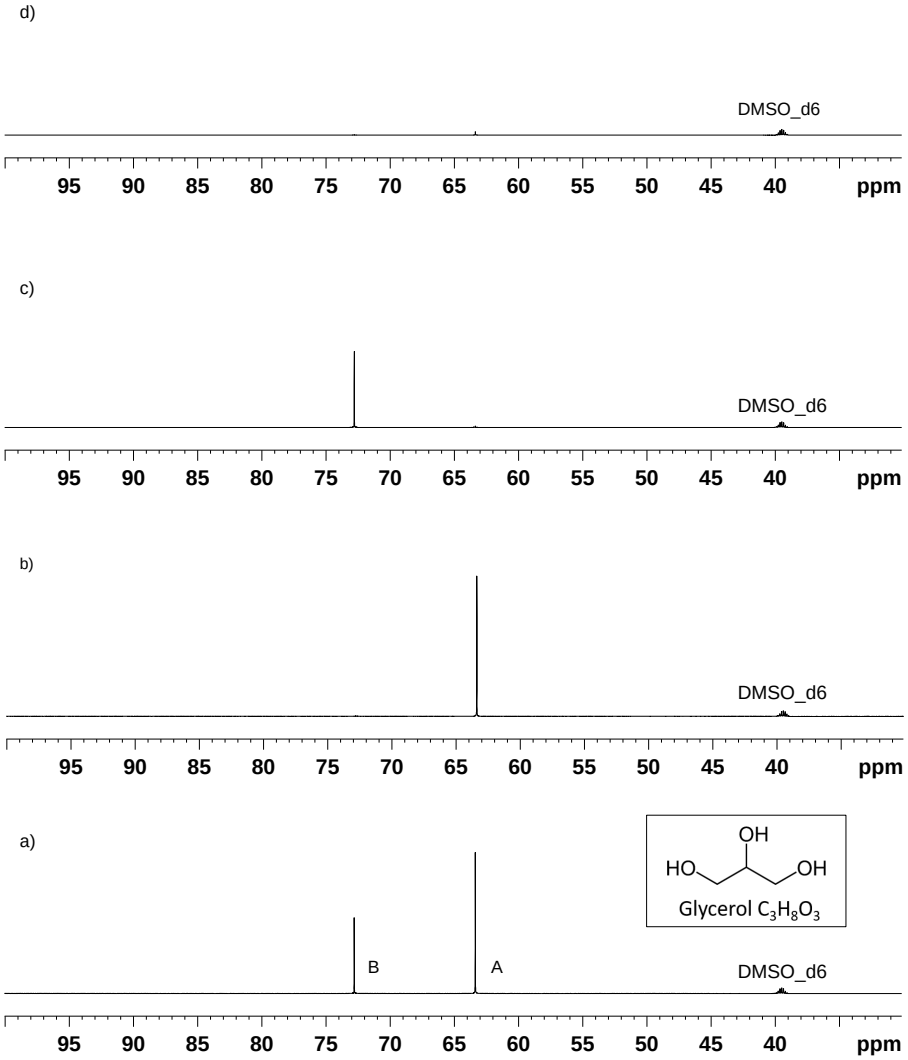

Figure 4. Presaturation of the glycerol. a) ^{13}C NMR spectrum of glycerol. Two signals A = 63.4 ppm and B = 72.8 ppm b) ^{13}C NMR spectrum of glycerol with single presaturation on A c) ^{13}C NMR spectrum of glycerol with single presaturation on B d) ^{13}C NMR spectrum of glycerol with multiple presaturation on A and B For the four analysis, NS = 8, DS = 4, P1 = 13.7 μsec, D1 = 3 sec. For the presaturated spectra, N = 50,000.

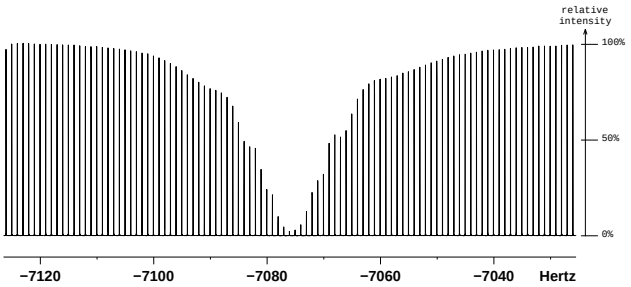

Figure 5. Measurement of the window for which presaturation causes a decrease of at least 50% of the signal A ($\delta = 63.4$ ppm) by modifying the auxiliary frequency in intervals of 1 Hz. The exact resonance of singal A is 10,279 Hz corresponding to an auxiliary frequency of 7,076 Hz.

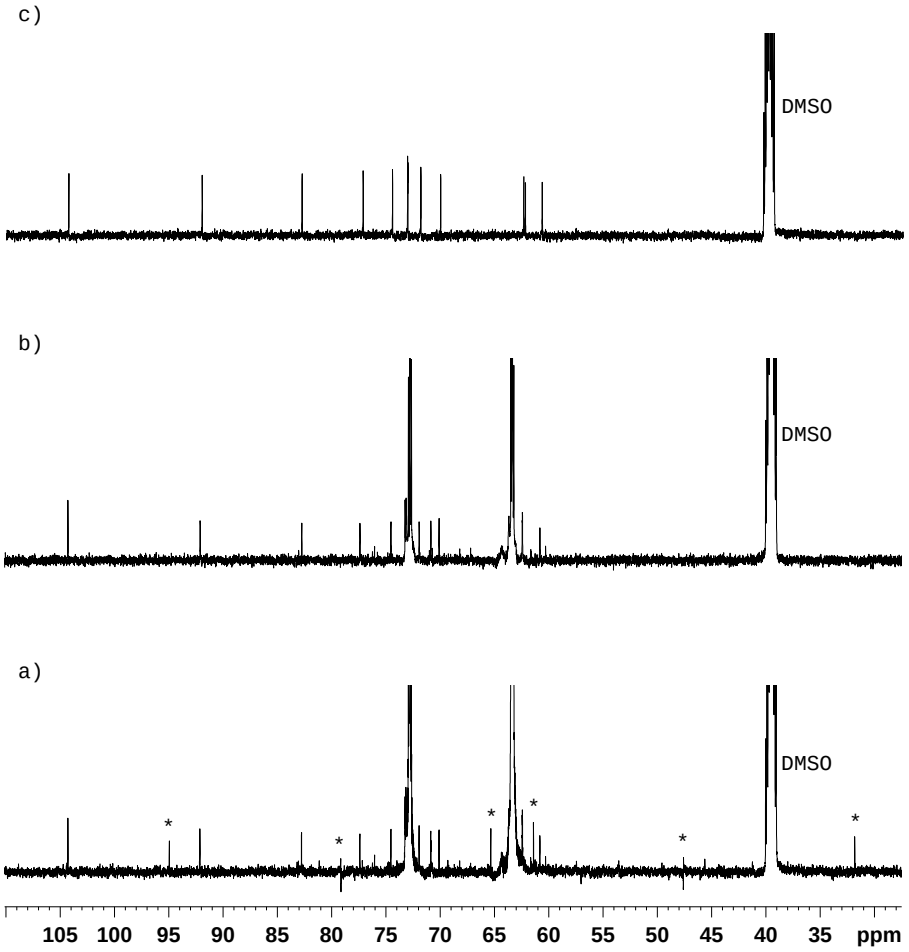

Figure 6. a)^{13}C NMR spectrum of sucrose (24 mM) diluted in glycerol (3.6 M) and DMSO–d_6. The "*" represent decoupling artifacts ; b) The same analysis with presaturation sequence ; c) ^{13}C NMR spectrum of sucrose (24 mM) in DMSO–d_6. For the three analysis, NS = 128, DS = 8, P1 = 13.7 μsec, D1 = 3 sec, N = 50,000

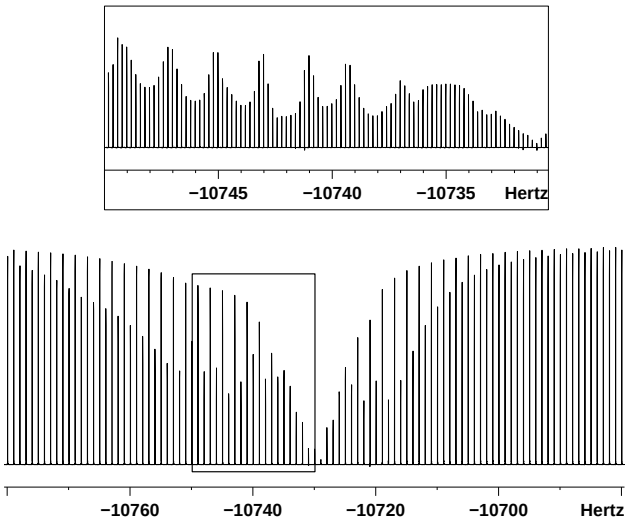

Figure 7. Unexpected presaturation profile in the region of two oxygen-bearing carbons for the 1,2–propanediol. A focus is made to make in evidence the wave profile.